Dark Matter in a single-metric universe

C. C. Wong
Department of Electrical and Electronic Engineering, University of Hong Kong. H.K.
(Dated: March 2, 2016)

A few years ago Baker proposed a metric, implementing the Bona-Stela construction, which interpolates smoothly between the Schwarzschild metric at small scales and the Friedmann-Robertson-Walker (FRW) metric at large scales. As it stands, by enforcing a homogeneous isotropic stress-energy tensor the predictions are incompatible with solar system data. We show that permitting a small radial inhomogeneity and anisotropy avoids this problem while introducing an effective dark matter (eDM) term that can go some way to explain flattened galactic rotation curves, the growth rate of the baryonic matter density perturbation and the enhancement of the higher CMB acoustic peak anisotropies.

PACS numbers: ??

arXiv:1601.00376v3 [astro-ph.CO] 1 Mar 2016

THE MODEL

The flattened nature of galactic rotation curves shows that if their matter is entirely visible then it does not obey Newtonian dynamics. The most common response is to assume that galaxies contain cold Newtonian dark matter (CDM), whose distribution can be inferred from the deviation of the rotation curves from those expected from the distribution of visible matter. However, to date, dark matter particles have not been found within our solar system [4]. Alternative approaches to explain dark matter without introducing new particles require modifying Newtonian dynamics (MOND) [5-9]. In its original formulation MOND is a phenomenological theory which is successful at galactic distances but becomes problematic at larger distances and at early epochs. The challenge is to provide a more fundamentally motivated relativistic frame-work which could account for the effects of dark matter where MOND is problematic.

In particular, we look for cosmological models connecting the static Schwarzchild metric in the presence of localised mass at small scales with the time dependent Friedmann-Le maître-Robsertson-Walker (FLRW) metric at large scales. The simplest way is to match the metrics [1-2] continuously at some (zero-pressure) interface. More realistically, to describe the motion of test particles in the vicinity of a point-mass M placed in an expanding cosmological background we follow Baker [1] in using a Lemaître-Tolman metric

$$ds^2 = -e^{2\alpha(\varrho,\tau)}d\varrho^2 - e^{2\beta(\varrho,\tau)}d\Omega^2 + c^2 d\tau^2 \tag{1}$$

with for proper time τ and comoving distance ϱ, with $d\Omega^2 = d\theta^2 + sin^2\theta d\varphi^2$,

Assuming spatial curvature is isotropic, $\theta = \frac{\pi}{2}$ and space is "flat", in our time-orthogonal system α can be chosen to satisfy $e^{\alpha} = \beta' e^{\beta}$ where $'$ denotes differentiation with respect to ϱ.

Different solutions of β represent different metrics. For example, $e^{\beta} = a(\tau)\varrho$, $e^{\alpha} = a(\tau)$ gives the Friedmann-Lemaître metric for scale factor a, while $e^{\beta} = R$, $e^{2\alpha} = r_s/R$, where R the proper distance and r_s the Schwarzschild radius leads to the Schwarzschild- Lemaître metric. The equation of motion depends solely on the choice of $\beta(\varrho,\tau)$.

We begin by repeating the analysis of [1]. With indices 1 and 4 denoting radial and temporal coordinates respectively, and $2, 3$ angular coordinates, Baker chose

$$8\pi T_1^1 = 2\frac{\ddot{\beta}}{c^2} + 3(\frac{\dot{\beta}}{c})^2 - \Lambda = 2\frac{\ddot{a}}{ac^2} + 3(\frac{\dot{a}}{ac})^2 - \Lambda, \tag{2}$$

where T^{μ}_{ν} is the stress momentum tensor and Λ is the cosmological constant. The left hand equation in (2) is the Einstein equation for the metric (1) and the right hand equation follows from the Bona-Stela construction in which they insert a spherical patch containing the mass M in a flat FLRW background.

Eq.(2) can be solved as

$$e^{\beta(\varrho,\tau)} = a(\tau)[C_1(\varrho) + C_2(\varrho)\omega_3(\tau)]^{2/3}, \ where \ \omega_\eta(\tau) = \int_{\tau_0}^{\tau} \frac{dt}{a(t)^\eta}. \tag{3}$$

and $C_1(\varrho)$, $C_2(\varrho)$ are arbitrary function of ϱ.

With $r = e^{\beta}$ the Newtonian (slow speed) limit of the equations of motion of a point mass at a proper distance r is given in detail by

$$\ddot{r} = \frac{\ddot{a}}{a}r - \frac{2C_2(\varrho)^2}{9a^3r^2} - \frac{2}{3}\frac{\dot{a}}{a}\frac{C_2(\varrho)}{(ar)^{3/2}}r + \frac{c^2C_0^2}{r^3}. \tag{4}$$

where $C_1(\varrho) = -C_2(\varrho)\varrho/c$ is chosen so that the $8\pi T_4^4$ goes to $3(\dot{a}/a)^2$ for large ϱ. We take $c^2C_0^2 = h^2$, where h is generally identified with constant angular momentum per unit mass of the system. In order to match Newton, we follow Baker's choice

$$C_2(\varrho) = -\frac{3}{2}\sqrt{2GM}. \tag{5}$$

where the negative sign is chosen to preserve the Schwarzschild-Lemaître singularity at $\varrho = c\omega(\tau)$ and M is the mass of the system at the centre of the spherically symmetric metric. See [1] for details. The model leads to the result

$$\ddot{r} = \frac{\ddot{a}}{a}r - \frac{GM}{a^3r^2} + \frac{\dot{a}}{a^2}\sqrt{\frac{2GM}{ar}} + \frac{h^2}{r^3}. \tag{6}$$

As Baker observed, this model is in disagreement with observations [1] because the additional a^3 factor in the Newtonian gravitational term implies a year length growing as $a^{9/2}$. We observe that the non-Newtonian term in (6) describes a repulsive force.

We shall now show that the additional a^3 factor in the Newtonian gravitational term is absent provided we take $\eta = 3/2$ in the choice of β in (3). This requires that (2) is replaced by the radially inhomogeneous

$$8\pi T_1^1 = 2\frac{\ddot{\beta}}{c^2} + 3(\frac{\dot{\beta}}{c})^2 - \Lambda = 2\frac{\ddot{a}}{ac^2} + (\frac{\dot{a}}{ac})^2 - \frac{2\dot{a}}{ac}\frac{\dot{\omega}}{(\varrho - c\omega_{3/2})} - \Lambda, \tag{7}$$

As before, we have chosen $C_1(\varrho) = -C_2(\varrho)\varrho/c$ is chosen so that $8\pi T_4^4$ goes to $3(\dot{a}/a)^2$ for large ϱ and have chosen C_2 as in (5) to match Newton. We also have

$$8\pi T_4^4 = 3\dot{\beta}\frac{\dot{a}}{a} - \Lambda \tag{8}$$

where an overdot means differentiation with respect to τ, where

$$\dot{\beta} = \frac{\dot{a}}{a} + \frac{2}{3}\frac{C_2\dot{\omega}}{(C_1 + C_2\omega)} = \frac{\dot{a}}{a} - \frac{2}{3}\frac{c\dot{\omega}}{(\varrho - c\omega_{3/2})} = \frac{\dot{a}}{a} + \frac{2}{3}\frac{C_2}{r^{3/2}}, \tag{9}$$

The Newtonian (slow speed) limit of the equations of motion of a point mass at a proper distance r is now given by

$$\ddot{r} = \frac{\ddot{a}}{a}r - \frac{GM}{r^2} - \frac{\dot{a}}{a}\sqrt{\frac{GM}{2r}} + \frac{h^2}{r^3} - \frac{3GMh^2}{c^2r^4}, \tag{10}$$

where the r^{-4} term is the relativistic correction and $h^2 = v^2r^2 = GMr$ is used in this term. Henceforth we shall ignore this term, reproducing (6) with the problematic a^{-3} factor removed. Here the non-Newtonian term describes an attractive force.

We note that $\frac{\dot{a}}{a} = H$ is the Hubble parameter governed by the Friedmann equations

$$(\frac{\dot{a}}{a})^2 = H^2 = \frac{8\pi G}{3}\rho + \frac{c^2\Lambda}{3} \tag{11}$$

where ρ is mass density of the background universe. The present value H_0 is given by [4].

$$\frac{\dot{a}}{a} \sim H_0 = 2.4 \times 10^{-18}s^{-1}. \tag{12}$$

We note that this relatively small value of H_0 introduces a scale below which the Newtonian acceleration dominates and a cutoff scale above which the FRW acceleration dominates. The potential that produces the acceleration in Eq. (10) is given by

$$V(r) = \frac{h^2}{2r^2} - \frac{GM}{r} + H\sqrt{2GMr} - \frac{1}{2}\frac{\ddot{a}}{a}r^2. \tag{13}$$

Before we explore whether the final term in (13) can be interpreted as effective Dark Matter (eDM), we observe that it comes with a cost for the isotropy of the energy-momentum tensor. Its angular components are related to its radial component by

$$8\pi T_2^2 = 8\pi T_3^3 = 8\pi T_1^1 + \frac{8\pi}{2\beta'}\frac{\partial T_1^1}{\partial \varrho}. \tag{14}$$

For $\eta = 3$ isotropy follows from (2), whereas for the $\eta = 3/2$ case above

$$8\pi T_1^1 - 8\pi T_2^2 = \frac{3}{2c^2}\frac{HC_2\dot{\omega}}{C_1 + C_2\omega} \approx -\frac{3H}{2c^2a^{3/2}}\frac{c}{\rho} \tag{15}$$

There is no surprise that, if we abandon radial homogeneity and (energy-momentum tensor) isotropy, the effect is to modify Newton's law for slowly moving material. To estimate the size of this anisotropy, we use the asymptotic limit of the metric which is the Schwarzschild-Lemaître condition in Eq. (3). For the Milky way parameters which are $a = 1$, $M = 3 \times 10^{42}$kg; the galactic radius $r \approx 6 \times 10^{22}$ m, we obtain the comoving distance scale

$$\frac{\varrho}{c} = \frac{r^{3/2}}{\sqrt{2GM}} = \frac{14.7 \times 10^{33}}{20 \times 10^{15}} = 0.735 \times 10^{18} s \tag{16}$$

and the anistropy is

$$8\pi T_1^1 - 8\pi T_2^2 \approx -0.85 \times \frac{\Lambda}{3} \tag{17}$$

At the edge of the Milky Way this anisotropy is a fraction of the Cosmological constant and decreases linearly as ϱ increases towards the cosmological scales where one recovers an effective isotropy and homogeneity. This anisotropy describes a pulling pressure towards the origin. We note that in Eq.(7) the value of ϱ implicitly depends on the parameters (C_1, C_2) in Eq.(3) and thus the "Cosmological principle" is valid at a scale sufficiently large from the scale of the nearest galaxy.

THE TULLY-FISHER RELATION, GALACTIC CUT-OFF SIZE AND DYNAMICAL MASS OF THE MILKY WAY

Using Eq.(10), we study the large distance effect the non-Newtonian term has on the rotational speed $v(r)$ of galactic dust in galaxies, where we assume the angular momentum effect is small.

$$v^2(r) = [\frac{GM(r)}{r^3} + \sqrt{\frac{GM(r)}{2r^3}}H - \frac{\ddot{a}}{a}]r^2 \tag{18}$$

One of the constraints for a reasonable modified gravity proposal is that it must satisfy the Tully-Fisher relation [see Ref. 5] which is given by

$$L \propto M \propto v_\infty^\alpha \tag{19}$$

where L is total luminosity, $v_\infty = lim_{r\to\infty}v(r)$ with $\alpha \approx 4$. The large distance limit of Eq. (18) is

$$v^4_{r\to r_H} = \frac{1}{2}GMcH_0 \tag{20}$$

where $r_H = c/H_0$ is the Hubble radius and it is clear that the eDM automatically satisfies the Tully-Fisher relation. For a point mass M approximation at the galactic centre, we note that when the distance approaches $r_c^3 \sim 2GM/H^2$ that the eDM term becomes significant. Thus as long as the galactic mass distribution is concentrated within a distance $r_0 \ll r_c$, a point mass approximation should be sufficient for Eq. (18) for large distances consideration at r_c. To estimate the size of the cut-off distance of Milky Way, we take our largest galactic mass estimate $\approx 3 \times 10^{42}$ kg (half of the M31 and Milky Way mass combined) and in Eq. (18) with $M(r) = M$ and write $\ddot{a}/a$ in terms of the deceleration parameter q, which is negative in the dark energy dominant epoch given by

$$\frac{\ddot{a}}{a} = -qH^2 \tag{21}$$

We estimate the cutoff value of r by solving Eq.(18) at $v^2 = 0$ and obtain

$$R^3_{cutoff} = \frac{8GM}{H^2(\sqrt{1-8q}-1))^2} \tag{22}$$

We note that in the matter dominant epoch where q is positive, there is no cut-off radius. From more empirical estimates, the deceleration parameter at the present epoch is given by $q(z \geq 0.09) = -0.34 \sim -0.38$ [Ref.10, Table II] whereas we have [3] $q_0 \approx -0.524$ based on the ΛCDM Planck estimate. To be model independent for now, we take the empirical values for now $q(z \geq 0.09) \approx -0.34 \sim -0.38$. The cut-off radius becomes

$$R_{cutoff} = 6.45 \sim 6.85 \times 10^{22} m \sim 2Mpc \tag{23}$$

where the observed general spiral galaxy halo radius is of order $10^{22}m$ [11]. This cut-off halo size will shrink as q decreases.

To estimate the dynamical mass of this eDM within a cutoff radius R_{cutoff}, we imagine that the eDM is some real matter and have a matter density around the centre of Mass of the galaxy. Putting the dark matter term in Eq. (10) on the same footing of baryonic matter, we have the total dynamical mass of eDM within a spherical shell as a function of r

$$M_{eDM} = H\sqrt{\frac{M_b r^3}{2G}};\ \ \rho_{eDM} = \frac{3H}{4\pi}\sqrt{\frac{M_b}{2Gr^3}} = \sqrt{\frac{3H^2}{8\pi G}}\sqrt{\rho_b}. \tag{24}$$

While the total eDM dynamical mass will increase until it reaches the cut-off radius, we note that eDM density will drop off as $1/\sqrt{r^3}$. Using the cutoff radius Eq.(22) we obtain a simple relation

$$\frac{M_{eDM}}{M_b} = \frac{2}{(1-8q)^{1/2}-1} \tag{25}$$

for q_0 range of value in Eq. (21) we find

$$M_{eDM} \approx 2.0 \sim 2.15 \times M_b. \tag{26}$$

This is consistent with the result, based on a study of around 1000 galaxies, of $M_{DM} \approx 1.5 \sim 2.0 M_b$ [12].The total mass of the Milky Way to luminous mass ratio is $3 \sim 3.15$. If the galaxy is in a sufficiently isolated region the matter density of the eDM in this region is then given by

$$\frac{\rho_{eDM}}{\rho_b} = \frac{2}{(1-8q)^{1/2}-1}. \tag{27}$$

THE EFFECT OF EDM ON MILKY WAY ACCRETION AND ROTATIONAL CURVES:

In the solar system we calculate the Mercury perihelion advance rate due to this eDM resulting in $\sim O(10^{-3})$ arcsec per century, which is much less than the 41 arcsec per century due to the relativistic correction term. Therefore the eDM effect will be insignifcant in solar system gravity considerations.

To see how the eDM affects the dust motions in a spiral galaxy such as the Milky Way, we study the simple case of the path of a particle mass m sufficiently far from the stellar disk of the galactic centre of mass M. We note that the unclosed orbital path for the particle having angular momentum $L = hm$ under the influence of a central potential with polar coordinate (r, φ) (e.g. see [13]) satisfies

$$\varphi - \varphi_0 = \int_{r_0}^{r} \frac{r^{-1}dr}{\sqrt{\frac{2}{h^2}(E/m - V)r^2 - 1}} \tag{28}$$

where E is the total energy. From the minimum of the potential V of (13), we note that the equilibrium distance between the angular momentum and the Newtonian potential is $r_{eq} = h^2/GM$, which is essentially the same as that of the full potential including the eDM potential since the eDM effective distance $r \sim (2GM/H^2)^{1/3}$ is far from r_{eq}. Eq.(28) becomes

$$\varphi - \varphi_0 = \int_{r_0}^{r} \frac{r^{-1}dr}{\sqrt{\frac{2}{h^2}(k/r + E/m - H_0\sqrt{2kr})r^2 - 1}}; \tag{29}$$

where $k = GM$. We follow the parametrisations in [12] by taking an appropriate length scale l with $h^2/(2k) = l$, and $r/l = \bar{\rho}$ and $y^2 = 1/\bar{\rho}$,

$$\varphi - \varphi_0 = -2 \int_{\frac{1}{\sqrt{2}}}^{y} \frac{dy}{\sqrt{1 - y^2 + E_0 y^{-2} - \lambda y^{-3}}}, \tag{30}$$

where $E_0 = (El)/(mk)$ and $\lambda = H_0\sqrt{2l^3/k}$ and we integrate only from distances larger than r_{eq}. We note that in Eq.(29, 30) that for $\lambda = 0$, $l = r_{eq}/2$ the orbits are the Keplerian, thus $r_{eq} = 2l$ becomes the largest scale where orbit remains strictly Newtonian. For non-zero λ, we need to know how far the non-Newtonian term remains small. Here we focus on the parameters of the Milky Way, the eDM potential term satisfies $\lambda/y^3 = H_0\sqrt{2/k}r^{3/2} < 1$ upto $\bar{\rho} = r/l \sim 200$ where the integrand in Eq. (29) is well defined, so that the eDM potential term can be treated as small for distances up to $\bar{\rho} \sim 200$. In the following we assume that we are dealing with the Milky Way. To understand the Eq.(30) in the range $2 \leq \bar{\rho} \leq 200$ we see that the intergral is hard to solve exactly, but we know we have the Keplerian solution for zero λ, so we make an expansion around small λ for the simplest case $E_0 = 0$,

$$\varphi - \varphi_0 \approx -2 \int_{\frac{1}{\sqrt{2}}}^{y} \frac{dy}{\sqrt{1 - y^2}} - \int_{\frac{1}{\sqrt{2}}}^{y} \frac{\lambda dy}{y^3(1 - y^2)^{3/2}} \tag{31}$$

both integrals in Eq.(31) can be intergrated, for large $\bar{\rho}$

$$\varphi - \varphi_0 = sin^{-1}(1 - 2/\bar{\rho}) + \frac{1}{2}\lambda\bar{\rho} + \lambda\frac{3}{4}\ln\bar{\rho} \tag{32}$$

Here for $\bar{\rho} \sim 200$ we have $1/\sqrt{\bar{\rho}}$ small, and $\lambda\bar{\rho}^{2/3} = \lambda_0 < 1$ nearly constant,

$$\varphi - \varphi_0 = \frac{\pi}{2} - \frac{2}{\sqrt{\bar{\rho}}} + \frac{1}{2}\frac{\lambda_0}{\sqrt{\bar{\rho}}} \tag{33}$$

Neglecting the phase angle, we have

$$\varphi = -\frac{2 - \lambda_0/2}{\sqrt{\bar{\rho}}} = -\frac{(2 - \lambda_0/2)\sqrt{l}}{\sqrt{r}} \tag{34}$$

which describes a hyperbolic spiral with narrower angular change from the Keplerian orbit for a large range of r near the cut-off scale. For $\bar{\rho} \sim 2$ and $r \sim r_{eq}$ the λ term in Eq. (31) approaches a constant$\times\lambda$ and can be absorbed into φ_0, and also we have $\lambda\bar{\rho}^{2/3} \ll 1$ in Eq.(29), one obtains for $\varphi_0 = \pi/2$ a Keplerian orbit

$$\bar{\rho} = \frac{2}{(1 - \epsilon cos\varphi)}; \quad r = \frac{r_{eq}}{(1 - \epsilon cos\varphi)} \tag{35}$$

where $\epsilon = \sqrt{1 + 4E_0}$ is the eccentricity of the Keplerian orbit. Starting from large $\bar{\rho}$ (and thus large r) at $\lambda = 0$ we recover an elliptic ($E < 0$) or parabolic ($E = 0$) path with the closest point to centre at $\bar{\rho} = 2$, or $r = r_{eq}$. For non-zero λ, Eq.(34) implies that for large $\bar{\rho}$ the dust will take a spiral path to move toward the centre of mass until $\lambda\bar{\rho}^{3/2}$ becomes small that Eq.(35) takes over and the dust will move in a Newtonian orbit. One effect of eDM is therefore to cause the baryonic matter from the large-distance halo region to follow a non-Keplerian spiral orbit into the rim of the Newtonian dominant region $r = r_{eq}$ so that here the matter density is of unusally high value due to matter accumulations.

Studies of the Milky Way is generally focussed on a central luminuous region described by a bulge consisting mainly of old stars and a stellar disk whose luminous density falls off sharply at around 13 kpc and becomes negligible at 16 kpc and the HI gas region outside the stellar disk. The Galactic Constants (GC) R_0 and V_0 are the sun's distance from and circular rotation speed around the galactic centre. At large scales, there are high velocity clouds (HVC) at 100 kpc to 1 Mpc with diameter ~ 15 kpc of typical mass at $3 \times 10^7 M_\odot$ moving towards the centre at high speed (eg. at 110 km/s for HVC at ~ 1 Mpc) [14]. These HVCs are thought to be caused by accretions which is now considered as a major feature in spiral galaxies causing the observed warps (an effect of accreting material whose net angular momentum is not parallel to that of the galaxy) outside stellar disk region. This accretion requires 10 times dark Newtonian particle as luminous matter. It is also clear that star-forming disk galaxies like the Milky Way needs to accrete $\gtrsim 1 M_\odot$ of fresh gas each year into their stellar disk and have built their disks gradually over the last 10

Gyr [15-16]. Thus the effect of accretions could have significant implications for the galactic matter composition and dynamics.
Modelling the mass densities of the Milky Way is still ongoing which includes modelling separately the stellar disk, the bulge and halo mass outside the stellar disk. For models of the stellar disk upto $r \sim 4R_0$, there are different approaches. The key ingredient is the Freeman model [17] which, with a key assumption of constant "mass to luminosity (M/L) ratio", is given by

$$\rho(r) = \rho_0 e^{-r/R_0} \tag{36}$$

where $\rho(r)$ is surface density function at distance r, ρ_0 is the central surface density. The Freeman formula for the rotational speed can be written as

$$v(r)^2 = 4\pi G\rho_0 R_0 y^2[I_0(y)K_0(y) - I_1(y)K_1(y)] = \frac{N^* M_s G r^2}{2R_0^3}[I_0(y)K_0(y) - I_1(y)K_1(y)] \tag{37}$$

$y = r/(2R_0)$, N^* the solar mass count, $M_\odot$ is the solar mass and I_0, I_1, K_0, K_1 are modified Bessel functions. For the Milky Way this Freeman formula matches closely the rotation curve observations and the Kelperian estimates up to the scale $r \approx 6$ kpc [Ref. 18, Table 2 and Ref. 19] and for larger distances such as $R_0 \approx 8$ kpc starts to fail to account for the flattening of the rotational curve. The failure of the Freeman model at these scales is generally assumed to be due to dark Newtonian particles. Within non-Newtonian gravity interpretation this failure can be addressed by a non-Newtonian term taking effect from $r > R_0$ such as Conformal gravity [20] and MOND [21] and produces a flatten rotational curve upto $r \sim 4R_0$ where the studies usually end.

Alternatively, one can show that the failure of the Freeman function at R_0 can be ascribed to a region of high M/L ratio from $R_0 \sim 4R_0$ [19] which claim visual support from the observed dark side-view of spiral galaxies. In ref. 19 by assuming that the gravitational forces are balanced against the centrifugal forces at each and every point in a finite series of concentric rings, fitting the observed rotation speeds profile one recovers a Freeman model mass density profile near the galactic centre but as one goes towards the edge of stellar disk the mass density behaves like Mestel model with higher M/L ratio. (the total luminuous mass estimate is 0.565×10^{42} kg at a distance of 30 kpc [19]) Similarly, the flatten rotation curves can be produced by the maximum disk model [22] in a study of 74 galaxies based on the van Albada and Sancisi hypothesis [23] that for "unknown reasons" that luminous matter aggregates maximally inside the stellar disk and bulge so that it can account for the rotational curves (and dark matter density if any would be highly constrained by luminuous matter density). In fact, the sufficiency of mass within the stellar disk to explain the rotation speeds are also found in Ref. 24-25. It would be important to look at the Milky Way rotational speed observations beyond $2R_0$, to this end we use the data from [Ref. 18 table 2] to plot the rotational speed of dust [see Figure 1a-1b]. From the data alone we observe that a peak of rotational speeds occurs around $9 \sim 30$ kpc ($R_0 \sim 4R_0$) but the speeds start to fall appreciably as distance grows. We note that the GC used here is $R_0 = 8.3$ kpc and $V_0 = 244$ km/s which is different from the more popular GC ($R_0 = 8.5$ kpc and $V_0 = 220$ km/s). The implication is the observed mass chosen at 16 kpc is higher than generally assumed. Also from Freeman [26], at 10 kpc the bulge is found to consist mainly ($\sim 80\%$) of very old stars of low "luminosity to mass" ratio, and these old stars also support a history of accretions towards the bulge from large distances clouds. From Eq. (18) we have $v^2(r) = \frac{GM(r)}{r}(1 + H\sqrt{r^3/2GM})$ where the second term (eDM factor) at 16 kpc is ~ 0.003 ($\sim 10^{38}$ kg) and is ~ 0.08 at 200 kpc. This means that at these scales for our model we can regard the derived mass from rotation speeds as efffectively coming from the luminous mass only. The above observations clearly support our central point mass analysis above where the Milky Way has a large halo region with matter accreting towards a robust central Newtonian region where the eDM is relatively weak.

The derived mass limit in Ref.18 is 1.328×10^{42} kg upto 189 kpc. We take the view that there is a high M/L accumulation around the bulge and the edge of stellar disk. At 16 kpc we take the mass estimate to be 0.76×10^{42} kg to match the rotational speed which peaks at ≈ 320 km/s, here we keep only the Newtonian attractive force and the eDM terms for simplicity, the effect of angular momentum will drop off faster as distance increases and the $\ddot{a}/a$ term will be small away from the cut-off radius. (A lower mass estimate say 280 km/s at 18 kpc will still yield a high $M(r) = 0.56 \times 10^{42}$ kg.) Outside the stellar disk, the HI gas mass is believed to be around 10% of total luminous mass within stellar disk. A simple central mass model could help us see how well Eq. (18) can describe the observations. Using Eq. (18) to plot rotational speeds away from 16 kpc and we see in Fig. 1a that the rotational speeds from Eq.(18) matches the observations extremely well upto 106 kpc, where the estimated mass is 0.89×10^{42} kg. Thus if we consider distances upto 106 kpc, a mass accumulation around 16 kpc and outside 16 kpc Eq.(18)

appears to be a good description of the rotational speeds without the presence of dark particles. We also note that there is a mass increase of 0.31×10^{42} kg between 106 kpc to 120 kpc leading to a jump in rotational curve. Using the derived mass from observation 1.2×10^{42} kg at 120 kpc as an input, at 189 kpc the rotation speed from Eq. (18) is 122 km/s vs 125 km/s from observations. This suggests that Eq. (18) can remain effective if one can account for the mass jump between 106 to 120 kpc. Thus luminous mass density information between 106 to 189 kpc will be important to understand whether rotation speeds require the input of dark particles or modified gravity. In Fig. 1b, we include two rotation speed limits for mass estimate below 2.0×10^{42} kg and 3×10^{42} kg upto 2 Mpc which is the cut-off distance given in Eq. (21). Here we expect an eDM induced flattening of rotational curve to show up from 600 kpc onward toward an upper bound value of 97 km/s. We see that the eDM primarily effects accretions of gas from large distances onto the stellar disk and bulge and also produce a flatten rotational curve at 600 kpc, but the well-known first flatten curve at $9 \sim 30$ kpc can be interpreted as due to the accumulation of (low luminosity) matter.

From [5] and [27-28] for X-ray groups and clusters of galaxies, the total mass to observable mass ratio can reach ≥ 7 which suggests the necessity of dark matter particles. We also note that in X-ray cluster calculations the dynamical mass estimate $M_N(r)$ for an isotropic isothermal sphere in hydrostatic equilibrium in [26] is proportional to the gas density ρ and temperature T at distance r from the centre of sphere:

$$M_N(r) = -\frac{krT}{G\mu m_p}[\frac{d\ln\rho}{d\ln r} + \frac{d\ln T}{d\ln r}] \tag{38}$$

where$k$ is the Botzmann constant, $\mu = 0.609$ and m_p is the proton mass. Eq. (36) is based on the equation

$$\frac{dP}{dr} = -\rho(r)\frac{GM(r)}{r^2}, \tag{39}$$

where P is the pressure in the gas. Therefore $M(r)$ in Eq. (37) should now include $M_{eDM}(r)$ from Eq. (22-23). However in the dark energy dominant epoch, from either best fit estimate [29] or a model with a cosmological constant, the deceleration parameter $q(z)$ will go to zero as $z \to z_T \approx 0.5$, where z_T is the transition point after which the dark energy begins its dominance. For $q \approx -0.05 \sim -0.1$, the total mass will increase to $6.85M_b \sim 11.92M_b$. However, precise determination of $q(z)$ value around z_T is not easy, for example for $z = 0.3$ the best fit models of [29] will give $q = -0.1 \sim -0.205$ with large error bars. Our analysis of the spiral galaxy above suggests that whenever there is high enough mass density concentration in the cluster, the eDM potential through accretions will increase the gas density distribution around a Newtonian dominant regime at some distance r_{eq}, this should also reduce the value of $M_N(r)$ estimate. Over time this mass accumulation should lead to higher $\rho(r)$ and therefore lowers the $M(r)$ estimate. Although we observe that Eq.(25,26,27) will fail for small q, in this case it simply means the cluster has no well defined cut-off.

DENSITY PERTURBATION EVOLUTION

At times before recombination, it is generally assumed that the overdense regions from inflation within the horizon will evolve into clusters of galactic objects. Dark collisionless particles will move into the centre of the perturbation both logarthmically in time during radiation epoch, and $\sim t^{2/3}$ during matter dominant epoch. The clumping of dark matter particles enhances the gravitational potential to assist baryonic matters to fall in faster after recombination. However, the eDM density in the matter dominant epoch is just a multiplicative factor of the uniform mass density and does not gravitate into the centre of perturbation before the recombination. To estimate the growth rate of small density perturbation in the matter dominant epoch under the influence of eDM, we note that the standard perturbation δ evolution equation is given by

$$\ddot{\delta} + 2H\dot{\delta} = 4\pi G\delta\rho \tag{40}$$

here the density perturbation δ is given by

$$\delta = \frac{\bar{\rho} - \rho}{\rho} \tag{41}$$

where $\bar{\rho}$ is the energy density of the overdense region of radius R, and ρ is the the background matter density. We use the standard derivations in [30] for the matter density of Eq. (18) the equation of motion for a point on the surface

R is now

$$\frac{\ddot{R}}{R} = -\frac{4\pi}{3}G\rho(1+\delta+\delta^{1/2}) \tag{42}$$

from Eq. (27) now the $\delta^{1/2}\rho$ term is the eDM density so that when $\delta = 0$ we recover the FRW solution. Here the total mass effective M within radius R is

$$M = (1+\delta+\delta^{1/2})\rho(\frac{4\pi}{3}R^3) \tag{43}$$

Here although the eDM is not baryonic and does not participate in the CMB temperature fluctuations, it directly affects the fluctuation growth of the baryonic density. We consider the case that the total mass (baryonic matter plus eDM) within the overdense region radius R remains constant over time whilst $R(t) = a(t)(1+\delta+\delta^{1/2})^{-1/3}$ grows as background density reduces. We should have $\delta+\delta^{1/2}$ in place of δ in Eq. (40). Without the eDM density $\delta^{1/2}\rho$, fluctuations grows most in the matter dominant epoch where $H = 2/(3t)$, and Eq. (40) becomes

$$\ddot{\delta} + \frac{4}{3t}\dot{\delta} - \frac{2}{3t^2}\delta = 0. \tag{44}$$

In a flat, matter-only universe where $a(t) \sim t^{2/3}$, the density pertubations will grow at the rate, given $\mid \delta \mid \ll 1$

$$\delta \propto t^{2/3} \propto a(t);\ \ a(t) \propto \frac{1}{1+z} \tag{45}$$

which leads to a growth $\delta \propto 10^3$ that is much less than the required total fluctuations growth of $\delta \geq 10^5$. As the eDM density is far larger than the matter density in Eq.(40), as an approximation we can replace δ by $\delta^{1/2}$ in Eq.(40) and Eq.(44) and obtain a new growth rate for δ as $\delta \propto t^{4/3} \propto a(t)^2$ which produces a growth rate of $\delta \propto 10^6$ since recombination. After recombination the baryonic density perturbation driven by the eDM will grow much faster than without the eDM, this could explain the large scale structure growth and Early Ionisation. The attractive background acceleration due to a large positive deceleration parameter q will also contribute.

We note from [31] that within the MOND approximation the first and second acoustic peaks in WMAP can be obtained with Baryonic matter alone. The lifting of the third compression peak is regarded as a major evidence for CDM since here baryonic matter alone is not enough to lift the odd peaks and MOND has no effect in the high acceleration region before recombination. The equation for the evolution of a single k-mode of the perturbation in density, δ, for fluctuation with small fractional amplitude is given by

$$\ddot{\delta}_k + 2H\dot{\delta}_k + \delta c_s^2 k^2 = 4\pi G\delta_k\rho \tag{46}$$

where c_s is the sound speed given by

$$c_s^2 = \frac{c^2}{3(1+\tilde{R})},\ \ \tilde{R} = \frac{3\rho_b}{4\rho_\gamma} \tag{47}$$

where ρ_γ is the photon density [32-33]. From the unperturbed Poisson equation, one replaces the term $-4\pi G\rho\delta$ by $k^2\phi_k$. The effect of the solution of Eq. (46) on the temperature fluctuations is

$$\frac{\Delta T}{T} = \phi_k + \frac{1}{3}\delta_k = \frac{(1+3\tilde{R})}{3}\phi_k cos(c_s kt) - \tilde{R}\phi_k \tag{48}$$

In the matter dominant epoch, from Eq. (22) we have

$$\rho_{eDM} = \delta^{1/2}\sqrt{\rho_b}\sqrt{\rho_b} = \frac{1}{\delta^{1/2}}(\delta\rho_b). \tag{49}$$

The matter potential ϕ_k is now dominated by the eDM term. Since the radiation density is not enhanced and baryons are still strongly coupled to photons. We can assume that the eDM only enhance the depth of the gravitational potential well while the photon-baryon fluid pertubation δ continues to drive the oscillations. Similar analysis in Eq. (46-48) suggests that the first and second peak should behave similarly to that of CDM and MOND. For higher peaks which enter the horizon earlier, we need to involve radiation. In the radiation dominant epoch, we have no immediate

guidance from previous sections on how the eDM will behave. As photon stress tensor has zero trace in a gravitational field, we expect that non-gravitating radiation density is not enhanced by the background density, we have

$$\rho_{eDM} = \delta^{1/2}\sqrt{\rho_b}\sqrt{\rho_\gamma} = \delta^{1/2}\rho_b\sqrt{\frac{\rho_\gamma}{\rho_b}} \tag{50}$$

which provides an increase of potential depth of $\sqrt{\rho_\gamma/\rho_b}$ from the matter dominant epoch and lifting the higher peaks in the radiation epoch,

$$\frac{\Delta T}{T} = \frac{(1+3\tilde{R})}{3}\sqrt{\frac{\rho_\gamma}{\rho_b}}\phi_k cos(c_s kt) - \tilde{R}\sqrt{\frac{\rho_\gamma}{\rho_b}}\phi_k \tag{51}$$

here $\tilde{R} \ll 1$. Thus in the radiation dominant epoch, it is clear that the eDM can play the role of external driving force and lift the higher acoustic peak without the baryon loading. This could provide the freedom to choose $\Omega_b h^2$ to be closer to the BBN value. We also notice that in Eq. (46) that when the sound speed c_s^2 is small after recombination, the eDM density from Eq. (49) is a factor of 100 to that of the Baryonic matter density and should provide a much stronger damping to the Baryon Acoustic Oscillations (BAO). This strong BAO suppression is a major problem for MOND. [34].

SUMMARY

The issues around the nature of dark matter remains unresolved. With no modification of Einstein Gravity, we find that in a Single-metric approach for a spherical symmetric region with central mass concentration in the FRW background to possess an eDM term in the slow speed limit of its particle equation of motion. This solution has no free parameter and the eDM term has a built-in dependence on the Hubble parameter. This eDM density can vary from being a large factor of an uniform mass density in an overdense region in the matter dominant epoch to becoming a massive halo density in the dark energy dominant epoch. We show how this new eDM term can account for some observations which motivate the need for dark Newtonian particles in different epochs and could provide answers for other difficulties that are not fully explained by the modified gravity approximation.

Acknowledgement: C.C.W thanks Prof. Ron. Hui, the Hong Kong University EEE Department for the support of this work and Prof. A. V. Tutukov for an useful communication.

NOTES

However, the deviations from the Schwarzschild metric are sufficient to put it in disagreement with the solar system data, essentially as a consequence of imposing radial-angular isotropy ($T_r^r = T_\theta^\theta$, etc.) in the energy-momentum tensor.

We examine the effects of dropping this condition. In the slow speed limit we find that the tradeoff in dropping isotropy to satisfy the data is to introduce an additional "effective dark matter" eDM term in the equation of motion. For a spherically symmetric system we find that this eDM becomes significant when the background energy density is comparable to the mass density. In a spiral galaxy, at large distances near a cut-off distance the eDM becomes dominant and behaves like a massive halo and predicts a flattened rotational curve. Using the estimates of the Milky Way, at smaller distances near a minimum potential "bulge" the eDM density is negligible in comparison to the visible mass density and the orbits are Newtonian. The effect of the eDM from the bulge to the cut-off distance is to provide a much steeper non-Newtonian potential that prevents matter from following the Keplerian orbits. Matter will follow a shorter spiral path to accrete around Newtonian dominant orbits. For the rotational curve observations in the Milky Way, based on a single higher mass to luminosity ratio around the bulge, the rotational curve matches the observations extremely well up to 100 kpc. This eDM term also predicts a non-Newtonian flattened rotational curve from 600 kpc up to the galactic cutoff. The total mass is estimated to be around 3 times the observable mass.

Further, during the early matter dominant epoch, in the presence of the eDM the baryonic matter perturbation growth rate is driven by the eDM and and grows as the square of its non-eDM rate and is thus fast enough to reach unity at low redshift and provide a natural mechanism for the large scale structure growth and early re-ionization. We also discuss how the eDM can lift the higher peaks observed in the CMB power spectrum. Where appropriate we comment on the eDM's effect on the dynamical mass increase in clusters of galaxies and the suppression of the Baryon Acoustic Oscillations.

References

1. G. A, Baker Jr., "Effects on the structure of the universe of an accelerating expansion" arXiv:astro-ph/0112320;
2. C. Dyer and C. Oliwa, "The "Swiss cheese" cosmological model has no extrinsic curvature discontinuity: A comment on the paper by G.A. Baker, Jr (astro-ph/0003152), arXiv:astro-ph/0004090v1.
3. P.A.R. Ade, N. Aghanim, C. Armitage-Caplan; et al. (Planck Collaboration) (22 March 2013) "Planck 2013 results. I. Overview of products and scientific results- Table 9" Astronomy and Astrophysics (submitted) 1303:5062. arXiv:1303.5062.
4. C. Moni Bidin, G. Carraro, R.A. Méndez, R. Smith, "Kinematical and chemical vertical structure of the Galactic thick disk II. A lack of dark matter in the solar neighborhood", arXiv:1204.3924, accepted for publication for the Astrophysical Journal.
5. A. Aguirre "Alternatives to Dark matter(?)" arXiv:astro-ph/0310572v2; "Dark matter in Cosmology" in "Dark matter in the Universe: Jerusalem Winter School for Theoretical Physics 1986-1987" pp.1-17.
6. T. Clifton, P.G. Ferreira, A. Padilla, C. Skordia, "Modified Gravity and Cosmology" arXiv:1106.2476v3, Physics Reports 513, 1 (2012), 1-189.
7. C. Skordia, "The Tensor-Vector-Scalar theories theory and its cosmology", arXiv:astro-ph/0903.3602v1.
8. S. McGaugh, "A tale of two paradigms: the mutual incommensurability of ΛCDM and MOND. arXiv:1404.7525, Canadian Journal of Physics 93,250 (2015); B. Famaey, S. McGaugh, "Challenges for Lambda-CDM and MOND", arXiv: 1301.0623, Proceedings of the Meeting of the International Association for Relativistic Dynamics, IARD 2012, Florence.
9. P. D. Mannheim, "Alternatives to Dark Matter and Dark Energy", arXiv:astro-ph/0505266v2, Prog. Part. Nuvl. Phys. 56 (2006) 340-445.
10. B. Gumjudpai, "Quintessential power-law cosmology: dark energy equation of state", arXiv:1307.4552v1, Mod. Phys. Lett. A, Vol. 28, No. 29 (2013) 1350122.
11. H. Hoekstra, H.Yee, M. Gladders, Proceedings for "Where's the matter? Tracing dark and and bright matter with the new generation of large scale surveys", Marseille, 2001, arxiv:astro-ph/0109514.
12. Y. I. Byrun, Ph.D Thesis, 1992, Australian National University.
13. J. Daboul, M. Nieto, "Exact, E=0, solutions for general power-law potentials. I Classical orbits". arXiv:hep-th/9408057, Phys. Rev. E52 (1955)4430.
14. J. Binney, " Accretion by Galaxies", arXiv:astro-ph.GA/0003195, ASP Conf Ser Vol 197, eds Combes, Mamon and Charmandaris, pp 107-114.
15. R. Sancisi, F. Fraternali, T. Oosterloo, T. van der Hulst, Astron. Astrophys. Rev. 15. 189-223 (2008).
16. M. Aumer, J. Binney, MNRAS397,1286-1301(2009).
17. K. C. Freeman, "On the disks of Spiral and S0 galaxies", Astrophys. J 160 (1970) 811-830.
18. P. Bhattacharjee, S. Chaudhury and S. Kundu, " Rotational Curve of Milky Way out to $\sim$ 200 kpc", arXiv:1310.2659v3, version accepted for publication in Apj.
19. J. Q. Feng, C. F. Gallo, " Galactic rotation described with thin-disk gravitational model", arXiv:astro-ph/0803.0556v1, 4 Mar 2008; "Galactic rotation described with various thin-disk gravitational models", arXiv: astro-ph 0804.0217v1.
20. P. D. Mannheim, J. G. O' Brien, " Galactic rotation curves in Conformal Gravity", arXiv:1211.0188.
21. B. Famaey, J. Binney, "Modified Newtonian Dynamics in the Milky Way", arXiv:astro-ph/0506723, MNRAS 363:603-608 (2005).
22. P. Palunas, T. B. Williams, "Maximum disk mass models for spiral galaxies", arXiv:astro-ph/0009161v1, A.J. Vol. 120 (2000) No. 6.
23. T. S. van Albada, R. Sancisi, Phi. Trans. Roy. Soc. Lon. A, 320 (1986) 405.
24. G. Bertin, " Dynamics of galaxies" Cambridge University Press, 2000.
25. M Creze, E. Chereul, O. Bienayme, C. Pichon, A&A, 329 (1998) 920.
26. M. Ness, K. Freeman, " The metallicity distribution of the Milky Way Bulge", arXiv:1511.07438.
27. R. Sanders, " Clusters of galaxies with Modified Newtonian dynamics", arXiv:astro-ph/0212293v1, Mon. Not. R. Astron. Soc., 000,000-000 (2002).
28. G. Angus, B. Famaey, D. Buote, "X-ray group and clsuter mass profiles in MOND: Unexplained mass in group scale", arXiv:0709.0108, accepted in MNRAS.
29 L. Xu, C. Zhang, B. Chang and H. Liu, "Reconstruction of deceleration parameter from recent cosmic observations", arXiv:astro-ph/0701519.
30. D. Erb,"University of Wisconsin Milwaukee, Astron401, lecture 36-37 ".

31. S. McGaugh, "Confrontation of MOND predictions with WMAP first year Data", arXiv:astro-ph/0312570, Astrophys. J. 611 (2004) 26-39.
32. W. Hu, N. Sugiyama, Astrophys. J 471(1996) 542.
33. W. Hu, S.Dodelson, Ann. Rev. Astron. Astrophys. 40:171-216, 2002, arXiv:astro-ph/0110414 .
34. S. Dodelson, "The Real Problem with MOND", arXiv:astro-ph.CO/1112.1320.

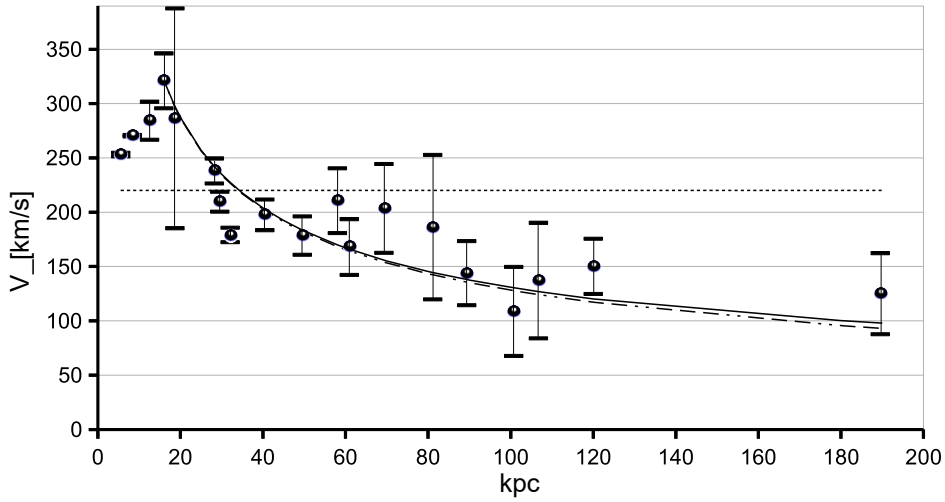

Figure 1a: Plot of the rotational speeds vs the distances from Milky Way centre, where the solid line is the results from Eq.(3.1) for mass at 0.76×10^{42} kg, the dashed line is the Newtonian speeds and the dots with error bars are the observational results from Ref.13 Table 2. The dotted line is a MOND estimate at $\upsilon = 220$ km/s.

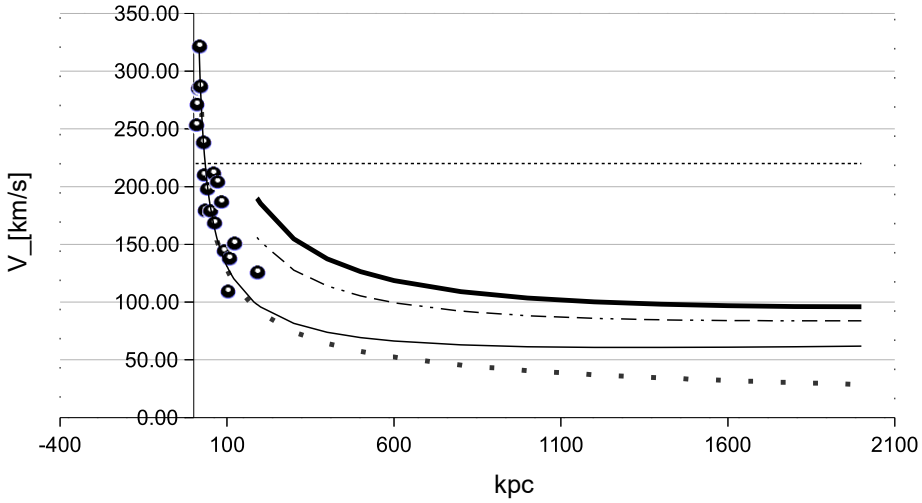

Figure 1b: Plot of the rotational speeds vs the distances from the Milky Way centre, where the thin solid line, the thin dashed line and thick solid line are the results from Eq. (3.1) for mass at 0.76×10^{42} kg and 2×10^{42} kg and 3×10^{42} kg respective-ly. The dots are the observational results from Ref.13 Table 2. The large dotted line is the Newtonian speeds for mass at 0.76×10^{42} kg and the fine dotted line is a MOND estimate at $\upsilon = 220$ km/s.